COMBINING OPTIAL-THERMAL REMOTE SENSING DATA AND TOPOGRAPHIC SLOPE FOR THE IDENTIFICATION OF DEBRIS-COVERED GLACIERS

Cheng Kou[1], Chunyang Zhao[1], Fan Yang[1], Jonathan Li[2], Yikun Liu[1], Fei Zeng[1]

1. Xi'an Surveying and Mapping Technological Center, China
2. University of Waterloo, Canada

ABSTRACT

Debris-covered glaciers are an important component of glacier systems on Earth. In this paper, using Landsat Thematic Mapper (TM) images, MOD05 products and digital elevation model (DEM) as data source. Land surface reflectance, land surface temperature (LST) and topographic slope are retrieved from optical bands, thermal band and DEM, respectively. A rule set that combines optical reflectance, LST and slope is proposed to identify debris-covered glaciers. The experimental results indicate that when introducing LST, the overall accuracy of identification increase by approximately 2.38% compared to that without using LST, and the majority of misclassifications of debris-covered glaciers are corrected.

Index Terms—Debris-covered glacier, optical-thermal remote sensing, topographic slope, Landsat Thematic Mapper (TM)

1. INTRODUCTION

Debris-covered glaciers account for a significant fraction of the global population of glaciers and are widespread in many mountain chains [1] in which landslide and rockfall hazards occur frequently. In high-relief mountain regions, debris-covered glaciers influence the regional-scale patterns of glacier length changes, mass balance and ice dynamics [2].

The objective of this study was to provide an inexpensive and effective method for identifying debris-covered glacier areas of mountain glaciers.

2. DATA AND METHODS

2.1. Data

Landsat-5 Thematic Mapper (TM) images with 30-m resolution (120 m for the thermal band) acquired on January 16, 2010 and Moderate Resolution Imaging Spectroradiometer (MODIS) Precipitable Water product (MOD 05) images with 1-km resolution acquired at the same date were used. Additionally, Shuttle Radar Topography Mission (SRTM) Digital Elevation Model (DEM) data with a 90-m resolution were used to do topographic correction and separate the shadow area and illumination area.

2.2. Retrieval of land surface reflectance and LST

The framework of our method is shown in Fig. 1. First, the land surface reflectance, land surface temperature (LST) and slope were retrieved from optical bands, thermal band and DEM data respectively. Second, some rules were established based on the analysis of random sample points. Finally, the TM image was classified using the rule set.

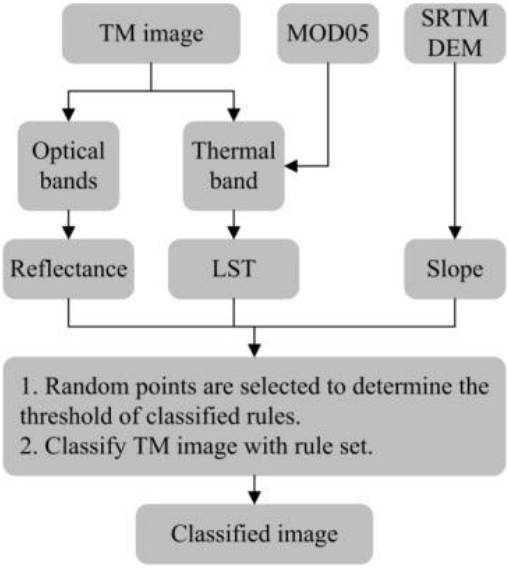

Fig. 1 Framework of the method.

The Fast Line-of-sight Atmospheric Analysis of Spectral Hypercubes (FLAASH) method [3] was used for atmospheric correction, and the improved topographic correction approach based on the classic C correction method [4] was applied for topographic correction. The thermal band of the Landsat TM image was used for LST retrieval with a generalized single-channel method ($SC^{JM\&S}$ algorithm) [5].

2.3. Classification with rule set

Some points were selected randomly over the study area and the features of every band (contains slope and LST feature) in every point was extracted. After analyzing the value of each band at every point, several rules were established to separate the different land. The threshold of every rule was selected manually.

3. EXPERIMENTS

A sub-basin of the Yigong Zangbo basin where located in the southern region of the Nyainqêntanglha Mountains was taken as the study area. The area covers 309.7 km^2, and the elevation ranges from 3,777 to 6,697 m above sea level (a.s.l.).

3.1. Establishment of classification rule set

Four land cover categories, clean glacier and snow, debris-covered glacier, bare rock and lake ice, were considered here. An abundance of shadow occurred in the study area, and therefore shadow was classified as a separate category. A certain extent of sand bank material was also observed around the river, and thus sand bank areas were classified as a unique category. A total of 240 sampling points were randomly selected (Table 1).

Table 1 Distribution of sample points for each land cover category*

LCC	GS	DG	BR	LI	SH	SB	Total
Number	75	47	30	37	19	32	240

*LCC=Land cover category, GS=Clean glacier and snow, DG=Debris-covered glacier, BR=Bare rock, LI=Lake ice, SH=Shadow, SB=Sand bank.

The processing steps are described as follows (Fig. 2):

(1) *If* $\rho_{Green} > 0.65$, *then pix* $\in$ *{GS, LI} else pix* $\in$ *{DG, BR, SH, SB}*

The reflectance of clean glacier and ice surfaces is higher than that of other categories. Hence, a threshold of 0.65 in the green band (Band 2 for TM) can be used to separate the clean glacier and snow and lake ice from other categories.

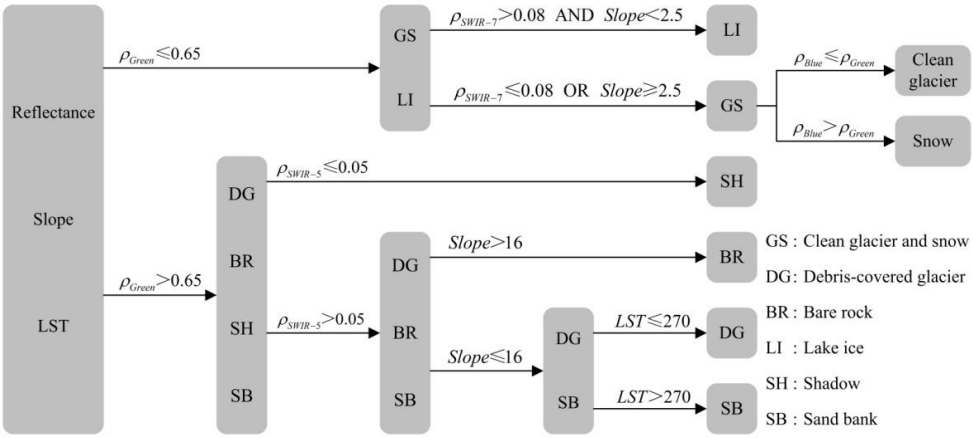

Fig. 2 Decision tree

(2) *If pix* $\in$ *{DG, BR, SH, SB} then (if* $\rho_{SWIR-5} > 0.05$, *then pix* $\in$ *{DG, BR, SB} else pix = SH)*

The reflectance of shadow surfaces is notably low in the SWIR band, and 0.05 was selected as a SWIR band threshold to separate shadow areas from debris-covered glacier and bare rock surfaces. In this study, we chose band 5, although another SWIR band (band 7) is also useful in this rule.

(3) *If pix* $\in$ *{GS, LI} then (if* $\rho_{SWIR-7} < 0.08$ *AND slope* < 2.5, *then pix = LI else pix = GS)*

The slope of lake ice is notably low, and its reflectance in the SWIR band (band 7 was used in this study) is concentrated within a small range (0.05-0.08). Therefore, lake ice and clean glacier and snow surfaces can be separated using the appropriate thresholds of band 7 and the slope.

(4) *If pix* $\in$ *{DG, BR, SB} then (if slope > 16, then pix = BR elseif slope < 16 AND LST > 270, then pix = SB elseif slope < 16 AND LST < 270, then pix = DG)*

Most of the bare rock is distributed within areas in which the slope is greater than 16°. Supraglacial debris formed from rockfalls or landslides can accumulate over long periods of time in areas where the slope is gradual, and therefore, the supraglacial debris was primarily distributed in areas where the slope is less than 16°. However, because the slope characteristic and spectral response of the sand bank surfaces is quite similar to those of the supraglacial debris, a certain extent of misclassification occurred for the sand bank areas (Fig. 5a). To correct these misclassified areas,

additional random points were selected for an improved analysis of the difference between supraglacial debris and the sand bank surfaces located in the gradual valleys. Temperature differences between these areas are likely to occur because supraglacial debris overlies glacial ice, which serves as a cooling source, whereas bare rock is devoid of any such cooling source located below its surface. Therefore, the LST feature could be used to correct the misclassified areas (Fig. 5b).

The clean glacier and snow surfaces could not be separated via visual interpretation, and therefore, sample points could not be selected over these two categories. However, the reflectance of snow (clean glacier) in the blue band (Band 1 for TM) is higher (lower) than in the green band [6]. This characteristic can be used to separate clean glacier and snow surfaces (Fig. 5c). Thus, a fifth rule was established:

(5) *If pix = GS then (if* $\rho_{Blue} > \rho_{Green}$*, then pix = Snow elseif* $\rho_{Blue} <= \rho_{Green}$*, then pix = Clean glacier)*

3.2. Accuracy assessment

To assess the accuracy of the classification results, 535 points were randomly selected over the entire study area. The assessment results are shown in Table 2.

Table 2 Accuracy assessment results

		GS	BR	DG	LI	SH	SB	OA*	Kappa
Without LST	PA (%)	89.67	80.95	88.31	52.38	97.83	0	86.73	0.82
	UA (%)	92.18	35.42	86.08	100.00	97.12	-		
With LST	PA (%)	89.67	80.95	88.96	52.38	97.83	58.82	88.79	0.85
	UA (%)	92.18	50.00	86.16	100.00	97.12	76.92		

*OA=Overall accuracy, PA=Producer's accuracy, UA=User's accuracy.

4. RESULTS AND DISCUSSION

4.1. Classification Accuracy

Without the use of LST information, sand bank and supraglacial debris surfaces could not be differentiated. When the LST data were included as a feature, the accuracy of the classification results increased. The majority of sand bank surfaces were correctly classified. Figure 3(b) shows that most of the sand bank surfaces that were misclassified as supraglacial debris surface without consideration of the LST feature were classified into the correct category when using the LST feature.

The supraglacial debris is primarily distributed in an area from the center to the terminal region of the glaciers, and the thickness of the cover debris increases closer to the terminal region. A greater abundance of bare rock is observed near the terminal region of glacier than around the upper region, and rockfall and landslide surfaces have occurred more frequently in these areas. Gradual terrain is suitable for the accumulation of debris, and more bare rock is located near the terminal region of the glacier than at the upper region. The glacier movement is expected to carry the debris towards the terminal end of the glacier.

4.2. Classification results

With our method, the study area is classified into seven categories (Fig. 3, Table 3).

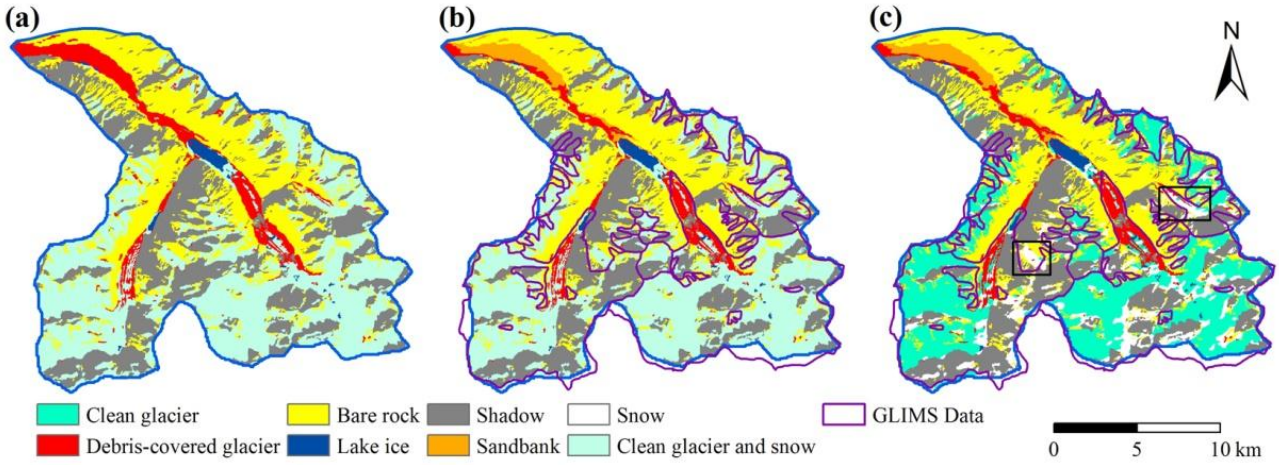

Fig. 3 Classification results: (a) without LST, (b) with LST and (c) separated clean glacier and snow.

If we compare our results with the glacier inventory from the GLIMS Database [7], the distribution trend of the glaciers appears similar. However, certain differences exist at the termini of the glaciers. The main reason for this difference may be that the date of analysis of the GLIMS Database is September 18, 2003, whereas the acquisition date of the TM images used in this study is January 16, 2010. These differences in the seasons and years between the two datasets may have led to variations in the observed distributions.

The fifth rule was able to differentiate between the clean glacier and snow surfaces, although certain glaciers were misidentified as snow (e.g., the black box in Fig. 3c). The reason for this discrepancy is that the image was acquired on January 16, i.e., during winter when snowfall may occur throughout the Yigong Zangbo basin and can cover the glaciers. When the GLIMS data were overlaid on our classification result, most of the snow was covered by the GLIMS data, and only 21.7% of snow (accounting for only 5.7% of clean glacier and snow surfaces) did not correspond to the GLIMS data. Additionally, the misclassification between clean glacier and snow surfaces did not affect the classification accuracy for debris-covered glacier surfaces, and therefore the error due to the misclassification between clean glacier and snow could be ignored.

Table 3 Area and proportion of each class in the study area

Category	Area (km^2)	Percentage (%)
Clean glacier	86.22	27.7
Debris-covered glacier	14.44	4.6
Bare rock	83.40	26.8
Lake ice	2.67	0.9
Sandbank	7.10	2.3
Snow	30.60	9.8
Shadow	86.71	27.9

5. CONCLUSIONS

In this letter, a classification method based on a rule set that combines optical-thermal remote sensing data and terrain slope was proposed for the identification of glacier surfaces, especially for debris-covered glaciers. The similarity of the optical band spectral responses from supraglacial debris and the adjacent periglacial debris, bare rock and sand bank hamper the accurate identification of debris-covered glaciers. The experimental results demonstrated the utility of the thermal band and topographic parameters for the identification of debris-covered glaciers. In addition, because of the characteristics of the rule set method, once the threshold of every rule set is selected the classification results of our method are stable and not dependent on the train samples.

The good quality and high spatial resolution DEM and thermal data may improve the accuracy of identification results.

6. REFERENCES

[1] C. D'Agata and A. Zanutta, "Reconstruction of the recent changes of a debris-covered glacier (Brenva Glacier, Mont Blanc Massif, Italy) using indirect sources: Methods, results and validation," *Global and Planetary Change,* vol. 56, pp. 57-68, 2007.

[2] L. Huang, Z. Li, B. Tian, J. Zhou, and Q. Chen, "Recognition of supraglacial debris in the Tianshan Mountains on polarimetric SAR images," *Remote Sensing of Environment,* vol. 145, pp. 47-54, 2014.

[3] E. A. C. Module, "QUAC and FLAASH User's Guide," *Atmospheric Correction Module, Version,* vol. 4, 2009.

[4] W. Huang, L. Zhang, and P. Li, " An improved topographic correction approach for satellite image," *Journal of Image and Graphics,* vol. 10, pp. 1124-1128, 2005. (in Chinese)

[5] J. C. Jiménez-Muñoz, J. Cristóbal, J. A. Sobrino, G. Sòria, M. Ninyerola, and X. Pons, "Revision of the single-channel algorithm for land surface temperature retrieval from Landsat thermal-infrared data," *Geoscience and Remote Sensing, IEEE Transactions on,* vol. 47, pp. 339-349, 2009.

[6] Q. Zeng, M. Cao, X. Feng, F. Liang, X. Chen, and W. Sheng, "A study of spectral reflection characteristics for snow, ice and water in the north of China," *Hydrological applications of remote sensing and remote data transmission,* vol. 145, pp. 451-462, 1984.

[7] R. Armstrong, B. Raup, S. J. S. Khalsa, R. Barry, J. Kargel, C. Helm, and H. Kieffer, *GLIMS glacier database*. Boulder, Colorado USA: National Snow and Ice Data Center, 2005.